



Aalborg Universitet

AALBORG UNIVERSITY
DENMARK

Degradation Effect on Reliability Evaluation of Aluminum Electrolytic Capacitor in Backup Power Converter

Zhou, Dao; Wang, Huai; Blaabjerg, Frede; Kær, Søren Knudsen; Hansen, Daniel Blom

Published in:

Proceedings of the 2017 IEEE 3rd International Future Energy Electronics Conference and ECCE Asia (IFEEC 2017 - ECCE Asia)

DOI (link to publication from Publisher):

[10.1109/IFEEC.2017.7992443](https://doi.org/10.1109/IFEEC.2017.7992443)

Publication date:

2017

Document Version

Accepted author manuscript, peer reviewed version

[Link to publication from Aalborg University](#)

Citation for published version (APA):

Zhou, D., Wang, H., Blaabjerg, F., Kær, S. K., & Hansen, D. B. (2017). Degradation Effect on Reliability Evaluation of Aluminum Electrolytic Capacitor in Backup Power Converter. In *Proceedings of the 2017 IEEE 3rd International Future Energy Electronics Conference and ECCE Asia (IFEEC 2017 - ECCE Asia)* (pp. 202-207). IEEE Press. <https://doi.org/10.1109/IFEEC.2017.7992443>

General rights

Copyright and moral rights for the publications made accessible in the public portal are retained by the authors and/or other copyright owners and it is a condition of accessing publications that users recognise and abide by the legal requirements associated with these rights.

- Users may download and print one copy of any publication from the public portal for the purpose of private study or research.
- You may not further distribute the material or use it for any profit-making activity or commercial gain
- You may freely distribute the URL identifying the publication in the public portal -

Take down policy

If you believe that this document breaches copyright please contact us at vbn@aub.aau.dk providing details, and we will remove access to the work immediately and investigate your claim.

Degradation Effect on Reliability Evaluation of Aluminum Electrolytic Capacitor in Backup Power Converter

Dao Zhou¹, Huai Wang¹, Frede Blaabjerg¹, Søren Kundsén Kær¹, and Daniel Blom-Hansen²

¹Department of Energy Technology
Aalborg University, Aalborg, Denmark
{zda, hwa, fbl, skk}@et.aau.dk

²Ballard Power Systems Europe
Hobro, Denmark
dbh@ballardeurope.com

Abstract - DC capacitors in power electronic converters are a major constraint on improvement of power density as well as reliability. In this paper, according to the degradation data of electrolytic capacitors through the accelerated test, the time-to-failure of the capacitor cell is acquired and it can be further extended to lower stress levels. Then, in a case study of a fuel cell backup power application, the mission profile based lifetime expectancy of the individual capacitor and the capacitor bank is estimated in terms of the standby mode and operation mode. The lifetime prediction of the capacitor banks can be obtained and compared with and without the degradation effect.

I. INTRODUCTION

Fuel cell system is emerging as an important candidate to substitute conventional technologies used in backup power application (e.g. generator set, or battery system), thanks to its high specific energy, high reliability, and no pollution [1], [2]. Due to the variable dc voltage with respect to the load current, the energy system based on fuel cell source needs to be regulated in order to achieve high-quality power supply [3]. Generally, the capacitor plays a vital role in the reliable operation of power electronic converters, which is one of the most susceptible elements to failure among other components [4].

The performance of electrolytic capacitor is complicated and highly affected by its operation conditions such as the voltage, current, frequency, and temperature. In addition, the electrolytic capacitor is also influenced by its degradation process. In the phase of degradation, the electrolytic liquid inside capacitor is gradually evaporated, which causes the rise of Equivalent Series Resistance (ESR) and the fall of the capacitance. Many researchers have investigated the degradation of the electrolytic capacitors [5]-[8]. For instance, a real-time failure detection method is developed for the changes of the ESR and capacitance of the capacitors [6]. Lifetime prediction models of electrolytic capacitors are established for the switch-mode power supplies and variable-frequency drivers [7], [8]. However, few studies investigate

the degradation effect on reliability evaluation considering the mission profile [9], [10], and this paper develops a physics-of-failure approach from the component-level [11]-[13] to system-level reliability that integrates the electrical modeling, thermal modeling, Weibull distribution, and reliability block diagram.

This paper addresses the reliability assessment of the capacitors used in a fuel cell system. Section II describes the basic structure of electrolytic capacitor and analyzes the tested degradation data. Mission profile based reliability evaluation approach is presented in Section III. Afterwards, Section IV investigates and compares the time-to-failure from the capacitor cell to capacitor bank whether the degradation effect is taken into account. Finally, the concluding remarks are drawn in last section.

II. DEGRADATION DATA OF ELECTROLYTIC CAPACITOR

A. Basic structure of electrolytic capacitor

Three types of capacitors are generally suitable for dc-link applications – the aluminum electrolytic capacitor, metallized polypropylene film capacitor and multi-layer ceramic capacitor, where the aluminum electrolytic capacitor is widely preferred due to the highest energy density and lowest cost per Joule [4]. Fig. 1(a) shows the configuration of the aluminum electrolytic capacitor, and it consists of an anode foil of pure aluminum, a layer of the insulating aluminum oxide (dielectric), electrolytic liquid, an air oxide layer, and a cathode foil. The liquid electrolyte (normally absorbed in the paper spacer) provides oxygen to re-form or self-heal the dielectric oxide layer.

The equivalent model of the electrolytic capacitor is shown in Fig. 1(b). C , R_s and L_s denote the capacitance, Equivalent Series Resistance (ESR) and the Equivalent Series Inductance (ESL), respectively. The dissipation factor is $\tan\delta = \omega R_s C$. R_p is the insulation resistance, denoting the condition of the leakage current. The widely used simplified capacitor model is composed of the capacitance, ESR, and ESL. It is worth noting that their values vary with temperature, voltage stress, frequency (i.e. operation conditions).

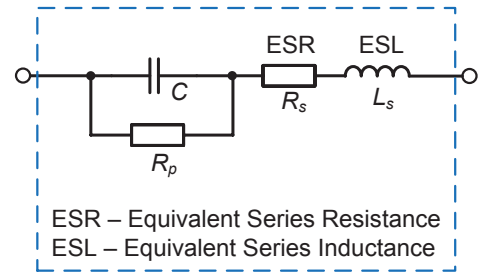
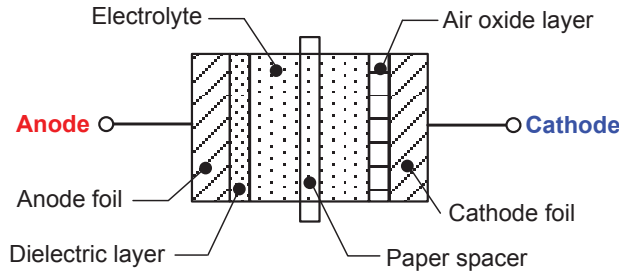


Fig. 1. Basic structure of aluminum electrolytic capacitor. (a) Configuration; (b) Equivalent circuit.

Basically, the electrolytic capacitor could fail due to the internal or external factors like design defect, material wear out, operating temperature, voltage, current, moisture and mechanical stress. The type of failure can be divided into the catastrophic failure due to single-event overstress and the wear-out failure due to the long-term degradation. For instance, in the case that the capacitor is exposed to intense vibration, the disconnection of the terminal may result in the failure mode of the open circuit. However, the evaporation of the electrolyte through a temperature-dependent drying-out process causes the wear-out issue, featuring the electrical parameters drift, such as the decrease of the capacitance, increase of the dissipation factor, and the increase of the leakage current.

B. Degradation data of electrolytic capacitor

In order to implement the accelerated degradation testing of the capacitor, the testing system is composed of a climatic chamber with a temperature range from -70°C to 180°C , a ripple current tester with DC voltage up to 500 V and AC current up to 30 A, and an LCR meter. Then, a degradation test is performed with a series of 9 capacitors ($680\ \mu\text{F}/63\ \text{V}$) at the rated voltage, rated ripple current ($2265\ \text{mA}/100\ \text{kHz}$), and upper operational temperature (105°C), where the normalized capacitance and ESR are regularly measured during 4,000 testing hours. As shown in Fig. 2, the degradation data is analyzed by using the software tool Reliasoft Weibull++ [9]. The decrease of capacitance and the increase of the ESR can be observed along with the testing hours. As the reduction rate of the capacitance increase significantly after 80% of its initial values, 20% of capacitance drop is considered as the end-of-life criteria, and the time-to-failure of each capacitor can be estimated.

By using the median rank (50% confidence level), the ranking of 9 failed capacitors can be calculated. Presented by the Weibull distribution [15], [16], the unreliability function is fitted in Fig. 3(a) with the shape factor β of 5.13 and the scaling factor η of 6,809. It is noted that the scaling factor denotes the characteristic life, i.e. the operation hour when 63.2% of the samples fail. As the B_X lifetime corresponds to the time when $X\%$ of the population fails, it is evident that 5000 hour lifetime stated in the datasheet roughly represents the B_{10} lifetime.

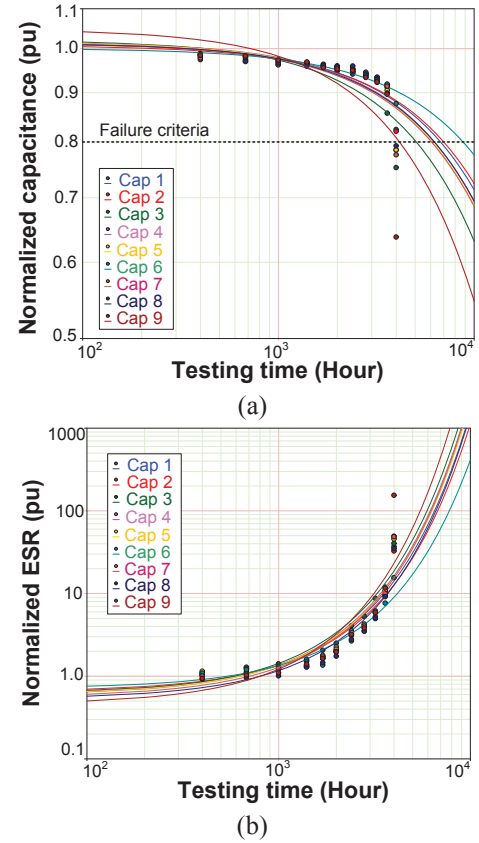


Fig. 2. Degradation results for 9 capacitors at the rated voltage, rated ripple current and upper operational temperature. (a) Normalized capacitance; (b) Normalized ESR.

C. Lifetime model of electrolytic capacitor

As discussed in [4], [17], a typical form of lifetime model of electrolytic capacitor is given by,

$$L(T) = L_0 \cdot 2^{\frac{T_0 - T}{n_1}} \left(\frac{V}{V_0}\right)^{-n_2} \quad (1)$$

where L_0 and L are the lifetime at the reference condition and the used condition, V_0 and V are voltage at the reference condition and the used condition, and T_0 and T are the temperature at the reference condition and the used condition,

respectively. n_1 is the temperature dependence constant, and n_2 is the voltage stress exponent. According to leading capacitor manufacturers [17], n_2 equals 0 for the small-size radial type capacitors if the applied voltage is below rated voltage, as the temperature-dependent electrolyte loss is the dominant failure mechanism. Meanwhile, n_1 equals 10. According to the above information, the time-to-failure at different temperature levels below the upper operation temperature can be estimated.

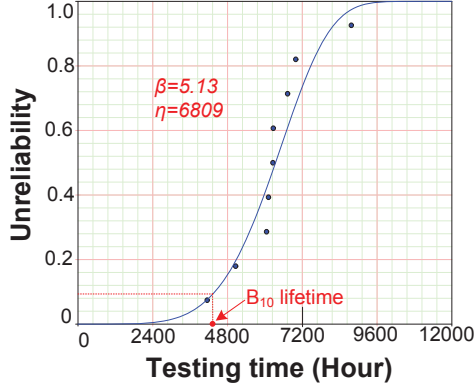


Fig. 3. Unreliability of capacitors along with operation time by using Weibull distribution.

III. MISSION PROFILE BASED RELIABILITY EVALUATION USED IN BACKUP POWER

A. Mission profile description of backup power converter

In order to cope with the wide-range output voltage of a fuel cell stack, a galvanic isolated power converter is applied as shown in Fig. 4, to supply a regulated output voltage for telecom applications. The electrolytic capacitors are used in the front-end and rear-end with the purposes of smooth input

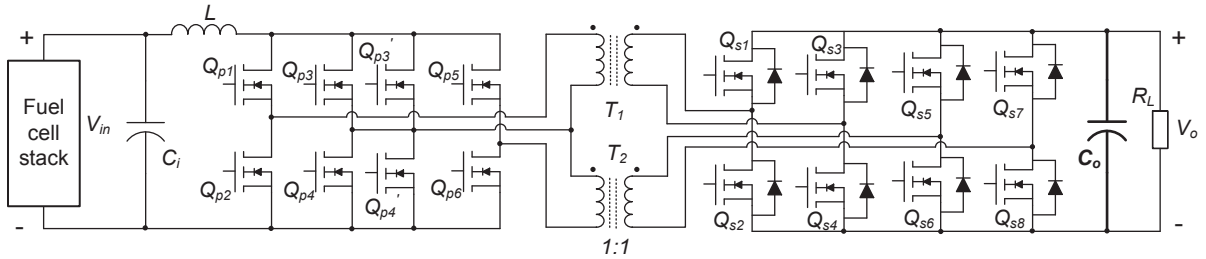


Fig. 4. Isolated dc/dc power converter used in fuel-cell backup telecom power.

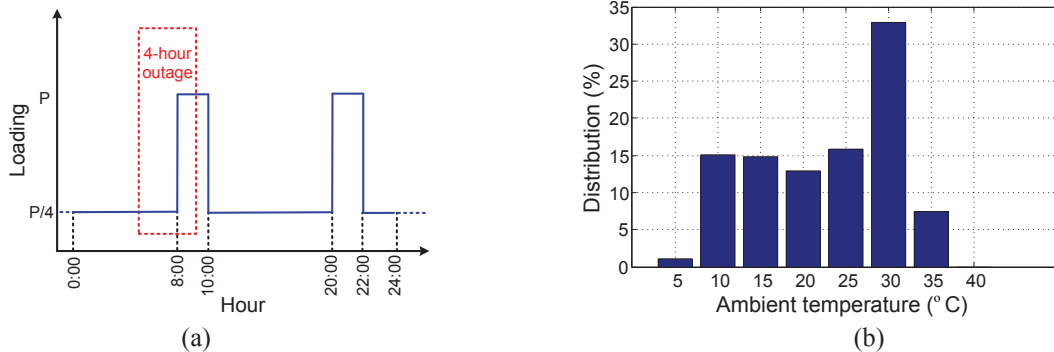


Fig. 5. Mission profile of the telecom backup power. (a) Loading profile and grid stability; (b) Ambient temperature distribution.

voltage and reasonable ripple of output voltage. To illustrate the reliability evaluation of the output capacitor bank C_o , composed by 8 electrolytic capacitors. It is worth noting that the lifetime of a single capacitor (component-level reliability) is considered in this section. Other key parameters of the power converter are listed in Table I.

Table I

POWER CONVERTER SPECIFICATION AND PARAMETERS

| | |
|------------------------------|-------------------------------|
| Maximum output power P_o | 1000 W |
| Input voltage V_{in} | 30 – 65 V |
| Output voltage V_o | 48 V |
| Primary-side MOSFETs | 100 V/74 A, $\times 8$ |
| Secondary-side MOSFETs | 100 V/74 A, $\times 8$ |
| Input capacitor C_i | 390 μ F/100 V, $\times 6$ |
| Output capacitor C_o | 680 μ F/63 V, $\times 8$ |
| Input inductor L | 15 μ H |
| Transformer ratio n | 1:1 |
| Switching frequency f_{sw} | 50 kHz |

In respect to the backup power application, two main working modes of the power converter can be identified. It mainly works in the standby mode in the case of the normal condition, while it is activated in the operation mode at the presence of the power outages. Consequently, the stability of the power grid is an essential mission profile. As shown in Fig. 5(a), a daily outage with 4-hour duration can be expected for severe users [3]. For the sake of simplicity, a typical telecom loading is periodically profiled with 10-hour full load and 2-hour quarter load [3]. As the ambient temperature affects the core temperature of the electrolytic capacitor, the annual temperature distribution is described in Fig. 5(b).

B. Approach to evaluate reliability of capacitors

The approach to evaluate the reliability metrics of electrolytic capacitor is described in Fig. 6, which is processed by the strength modeling, stress analysis, and reliability evaluation. In the phase of the strength modeling, as stated in Section II, the Weibull distribution of failed capacitors can be obtained at upper temperature range by using the accelerated lifetime testing. It can be further extended to lower temperature conditions with Arrhenius relation. Meanwhile, the degradation value of the capacitance and ESR can be recorded.

Then, the mission profile based thermal stress of the capacitor can be estimated depending on the grid stability. The core temperature of the capacitor is roughly the same with

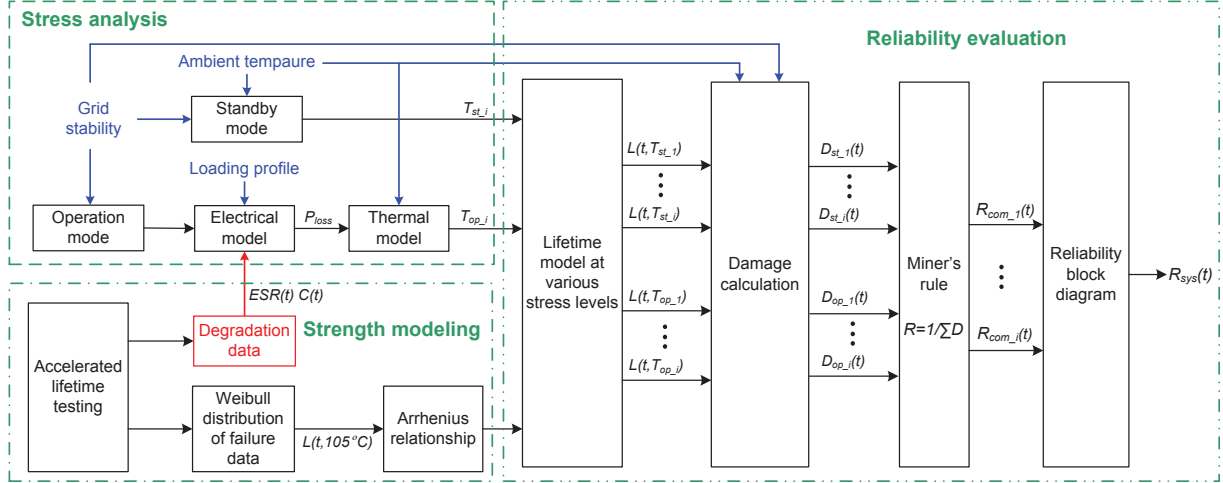


Fig. 6. Mission profile based reliability assessment of electrolytic capacitors used in backup power application.

IV. RELIABILITY ASSESSMENT FROM SINGLE CAPACITOR TO CAPACITOR BANK

In the case of the standby mode, the core temperature of the capacitor T_{st} is almost the same with the ambient temperature. The damage at each temperature is initially calculated by the annual operation hours at this thermal stress over the predicted hours that the capacitor can endure at this stress level. According to Miner's rule, each thermal stress has the same effect on degradation of the capacitor, and the annual damage D_{st} can be obtained by the sum of the damage at every ambient temperature.

$$D_{st} = \sum_{i=1}^7 \frac{P_{st} \cdot 365 \cdot 24 \cdot P_{Ta=i}}{L(T_{st,i})} = \frac{P_{st} \cdot 365 \cdot 24}{L_0} \sum_{i=1}^7 \frac{P_{Ta=i}}{2^{\frac{T_0 - T_{st,i}}{10}}} \quad (2)$$

where P_{st} denotes the percentage of the power converter working in the standby mode. P_{Ta} and L denote percentage of the ambient temperature distribution, and the predicted lifetime at the temperature level of T_{st} , which can be further calculated by (1). The subscript i indicates the temperature range from 5 °C to 35 °C as shown in Fig. 5(b).

ambient in the case of the standby mode, while it is jointly determined by the loading profile and the ambient temperature during the operation mode. The decreasing capacitance and increasing ESR may affect the core temperature of the capacitor.

Afterwards, the time-to-failure of capacitor can be calculated with different ambient temperature ranges at the standby mode and the operation mode, respectively. Annual damage can be obtained with the knowledge of the core temperature distribution throughout the whole year. The lifetime distribution of each capacitor can be calculated by using the Miner's rule. Finally, if the reliability block diagram is introduced, the component-level reliability of each capacitor forms the system-level reliability of the capacitor bank.

In the case of the operation mode, the loss dissipation of the capacitor is caused by the ripple current across the ESR. Then, the temperature rise of the capacitor can be estimated based on its thermal impedance and cooling solutions. As listed in Table II, the temperature rise of the input capacitor is 13.0 °C.

Table II
PARAMETERS RELATED TO CORE TEMPERATURE ESTIMATION OF THE USED CAPACITORS

| | | |
|---|------------------|------------|
| Output capacitor | Type | EEUFC1J681 |
| | Dimension | 12.5×35 mm |
| | Initial ESR | 141 mΩ |
| | Temperature rise | 13.0 °C |
| Thermal resistance from core to case | | 8.33 °C/W |
| Thermal resistance from case to ambient | | 18.15 °C/W |

Similar as (2), the annual damage at the operation mode D_{op} can be calculated as,

$$D_{op} = \sum_{i=1}^7 \frac{P_{op} \cdot 365 \cdot 24 \cdot P_{Ta=i}}{L(T_{op,i})} = \frac{P_{op} \cdot 365 \cdot 24}{L_0} \sum_{i=1}^7 \frac{P_{Ta=i}}{2^{\frac{T_0 - T_{op,i}}{10}}} \quad (3)$$

where P_{op} denotes the percentage of the power converter working in the operation mode. L denotes the predicted lifetime at the temperature level of T_{op} .

In order to investigate the standby and operation mode effects on the lifetime consumption, the B_1 , B_5 , and B_{10} annual damage is evaluated in Fig. 7 in terms of various temperature

ranges. It can be seen that the standby mode consumes higher damage compared to the standby mode, due to the fact that in spite of the higher core temperature in the case of the operation mode, the power converter mainly works in the operation mode. Meanwhile, it is obvious that higher B_X value results in lower total annual damage.

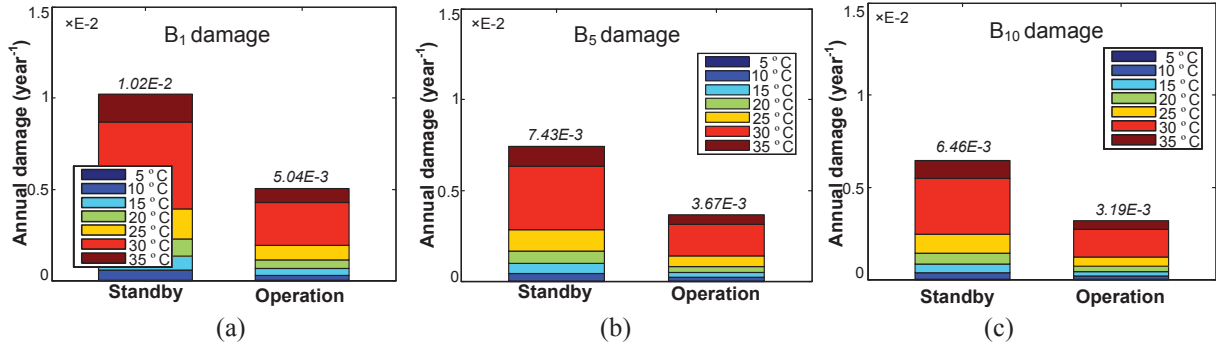


Fig. 7. Annual damage at the standby mode and the operation mode. (a) B_1 damage; (b) B_5 damage; (c) B_{10} damage.

A failure occurs in the situation that the accumulated damage reaches 1, which increases normally linear along with the year. However, the core temperature of the capacitor can gradually become higher due to the degrading ESR and capacitance. As shown in Fig. 8, the accumulated damage at various operation modes is analyzed and compared whether

the degrading data is taken into account or not. It can be seen that the degradation affects in the operation mode, as the capacitor temperature is the same with ambient in the standby mode. The B_1 lifetime of the capacitor decreases from 66 to 62 years if the degradation effect is taken into account.

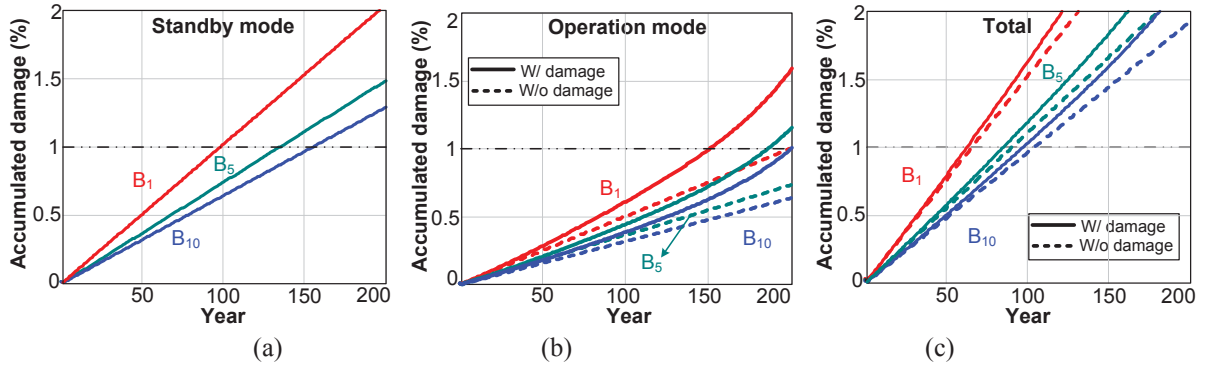


Fig. 8. Accumulated damage at various operation modes considering degradation data or not. (a) Standby mode; (b) Operation mode; (c) Both standby mode and operation mode.

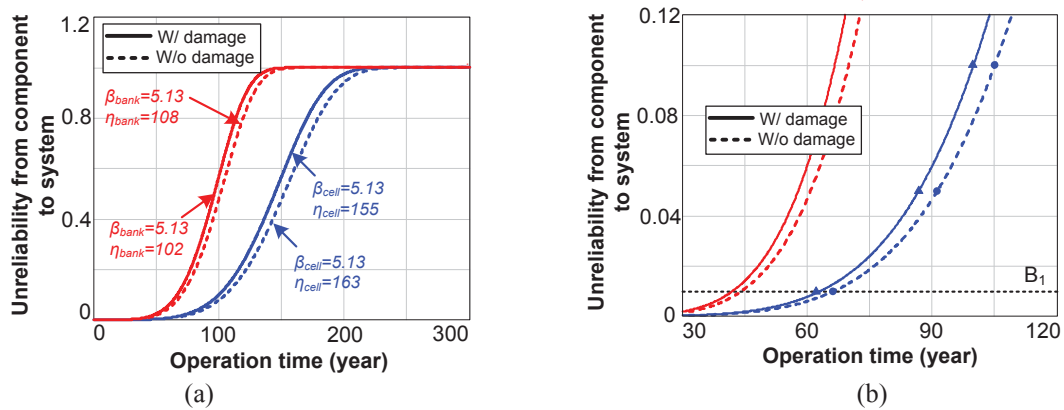


Fig. 9. Time-to-failure from capacitor cell to capacitor bank with and without the degradation. (a) Overview; (b) Zoom-in.

On the basis of the total accumulated damage of the single capacitor, its Weibull distribution of time-to-failure can be fitted as shown in Fig. 9. Same shape values of Weibull function can be found due to the identical failure criteria, and the scaling factor shrinks from 163 to 155 due to the annually increasing ESR. As the capacitor bank is composed of 8 independent capacitor cells, the reliability function of the capacitor bank is the product of the whole capacitor cells according to the theory of the reliability block diagram. In this reliability-critical application of the backup power, it is noted that the B_1 lifetime of the capacitor bank is estimated at 44 years compared to 66 years of the capacitor cell. Moreover, if the degradation effect is taken into account, B_1 lifetime further reduces to 42 years.

V. CONCLUSION

In respect to the power conditioning stage of the fuel cell stack used in backup power application, the degradation effects on the reliability metrics of the capacitor cell and the capacitor bank have been studied and evaluated in this paper. On the basis of the accelerated testing of the electrolytic capacitors in the condition of the severe thermal stress level, their degrading data and the time-to-failure distribution can be obtained. The lifetime distribution of the capacitors can be extended to the lower stress levels according to Arrhenius relations. With the approach of the mission profile based reliability evaluation of the capacitors, the annual damage of the standby mode and operation mode is investigated. As the degrading capacitance and equivalent series resistance affect the thermal loading, the total annual damage can be compared with or without the degradation. It is evident that the degradation effect results in the decreased B_1 lifetime of the capacitor cell from 66 to 62 years. From the viewpoint of the system-level reliability, the B_1 lifetime of the capacitor bank reduces from 44 to 42 years whether the degradation effect is taken into account.

References

- [1] K. Rajashekara, "Hybrid fuel-cell strategies for clean power generation," *IEEE Trans. on Industry Applications*, vol. 41, no. 3, pp. 682-689, May 2005.
- [2] M. Jang, and V. G. Agelidis, "A minimum power-processing-stage fuel-cell energy system based on a boost-inverter with a bidirectional backup battery storage," *IEEE Trans. on Power Electronics*, vol. 26, no. 5, pp. 1568-1577, May 2011.
- [3] M. J. Vasallo, J. M. Andujar, C. Garcia, and J. J. Brey, "A methodology for sizing backup fuel-cell/battery hybrid power systems," *IEEE Trans. on Industrial Electronics*, vol. 57, no. 6, pp. 1964-1975, Jun. 2010.
- [4] H. Wang, and F. Blaabjerg, "Reliability of capacitors for DC-link applications in power electronic converters—an overview," *IEEE Trans. on Industry Applications*, vol. 50, no. 5, pp. 3569-3578, Sep. 2014.
- [5] B. Sun, X. Fan, C. Qian, and G. Zhang, "PoF-simulation-assisted reliability prediction for electrolytic capacitor in LED drivers," *IEEE Trans. on Industrial Electronics*, vol. 63, no. 11, pp. 6726-6735, Nov. 2016.
- [6] K. Abdennadher, P. Venet, G. Rojat, J. M. Retif, and C. Rosset, "A realtime predictive-maintenance system of aluminum electrolytic capacitors used in uninterrupted power supplies," *IEEE Trans. on Industry Applications*, vol. 46, no. 4, pp. 1644-1652, Jul. 2010.
- [7] A. Lahyani, P. Venet, G. Grellet, and P. J. Viverge, "Failure prediction of electrolytic capacitors during operation of a switch-mode power supply," *IEEE Trans. on Power Electronics*, vol. 13, no. 6, pp. 1199-1207, Nov. 1998.
- [8] M. L. Gasperi, "Life prediction modeling of bus capacitors in ac variable frequency drives," *IEEE Trans. on Industry Applications*, vol. 41, no. 6, pp. 1430-1435, Nov. 2005.
- [9] D. Zhou, H. Wang, and F. Blaabjerg, "Lifetime estimation of electrolytic capacitors in a fuel cell power converter at various confidence levels," in *Proc. of SPEC 2016*, pp. 1-6, 2016.
- [10] D. Zhou, F. Blaabjerg, T. Franke, M. Tonnes, and M. Lau, "Reduced cost of reactive power in doubly fed induction generator wind turbine system with optimized grid filter," *IEEE Trans. on Power Electronics*, vol. 30, no. 10, pp. 5581-5590, Oct. 2015.
- [11] D. Zhou, F. Blaabjerg, M. Lau, and M. Tonnes, "Optimized reactive power flow of DFIG power converters for better reliability performance considering grid codes," *IEEE Trans. on Industrial Electronics*, vol. 62, no. 3, pp. 1552-1562, Mar. 2015.
- [12] K. Ma, H. Wang, and F. Blaabjerg, "New approaches to reliability assessment: using physics-of-failure for prediction and design in power electronics systems," *IEEE Power Electronics Magazine*, vol. 3, no. 4, pp. 28-41, Dec. 2016.
- [13] H. Oh, B. Han, P. McCluskey, C. Han, and B. D. Youn, "Physics-of-failure, condition monitoring, and prognostics of insulated gate bipolar transistor modules: a review," *IEEE Trans. on Power Electronics*, vol. 30, no. 5, pp. 2413-2426, May. 2015.
- [14] Reliasoft Corporation, "Life data analysis reference," [Online]. Available: www.reliasoft.com, 2016.
- [15] P. D. T. O'Connor, and A. Kleyner, *Practical Reliability Engineering (fifth edition)*. New York, USA: Wiley, 2012.
- [16] H. S. Chung, H. Wang, F. Blaabjerg, and M. Pecht, *Reliability of power electronic converter systems*. Institution of Engineering and Technology, 2015.
- [17] A. Albertsen, "Electrolytic capacitor lifetime estimation – key parameters are necessary to predict lifetime," *Bodo's power systems*, Apr. 2012.